

# IMAGE ENHANCEMENT AND MOTION COMPENSATION OF MOVING TARGETS IN ISAR USING S-METHOD

Thayananthan Thayaparan

Defence R&D Canada

Ottawa, Ontario, Canada

Thayananthan.Thayaparan@drdc-rddc.gc.ca

Ljubiša Stanković, Miloš Daković, Igor Djurović,

Vesna Popović

University of Montenegro

Podgorica, Montenegro

{ljubisa, milos, igordj, pvesna}@ac.me

**Abstract**—For target recognition applications, a blurred ISAR image has to be refocused quickly so that it can be used for real-time target identification. In this paper, we present the S-method-based approach to real-time motion compensation, image formation and image enhancement of moving targets in ISAR. This approach performs better than the Fourier transform by drastically improving images of fast, maneuvering targets. The method is also computationally simple, requiring only slight modifications to the existing Fourier transformbased algorithm.

**Keywords:** ISAR images, Motion Compensation, S-method, Fourier Method, Time-Frequency Analysis

## I. INTRODUCTION

In this paper we propose that the S-method-based calculation be used [1, 2]. As with the Wigner-Ville distribution (WVD), the S-method can produce concentrated representations of linear frequency changes and has the added advantage of being cross-term free (or with significantly reduced cross-terms). In contrast to other reduced interference distributions, which are usually derived under the condition that the marginal properties are preserved (what inherently leads to auto-term degradation with respect to the WVD [3]), the S-method is derived with the goal of preserving the same auto-terms as in the WVD, while avoiding cross-terms [4, 5, 6]. In other words, the method automatically compensates for quadratic and all even higherorder terms in phase induced by the target’s complex motion, leading to well-focused images. The S-method is also numerically very simple and requires just a few more operations than the standard Fourier transform-based algorithm. This method works on the whole set of data and it does not split the ISAR image into a time series of ISAR images, as in the case of common time-frequency techniques. These are significant advantages over other quadratic representations and over linear transforms based on signal dechirping and multiparameter search procedures.

## II. ANALYTIC CW RADAR SIGNAL MODEL

For the analytic derivation of the model, consider a continuous wave (CW) radar that transmits a signal in the form of a coherent series of chirps [7]:

$$v_p(t) = \begin{cases} \exp(j\pi Bf_r t^2) & \text{for } 0 \leq t \leq T_r \\ 0 & \text{otherwise,} \end{cases} \quad (1)$$

where  $T_r$  is the repetition time,  $f_r = 1/T_r$  is the repetition frequency, and  $B$  is the emitted waveform bandwidth. In one revisit, the transmitted signal consists of  $M$  such chirps:

$$v(t) = \exp(-j\omega_0 t) \sum_{m=0}^{M-1} v_p(t - mT_r), \quad (2)$$

where  $\omega_0$  is the radar operating frequency. The total signal duration is  $T_c = MT_r$  and represents the CIT (coherent integration time). Consider a signal of (2) transmitted toward a target. If the target distance from the radar is  $d$ , then the received signal is delayed with respect to the transmitted signal by  $t_d = 2d/c$  where  $c$  is speed of light. The phase of the received signal is changed as

$$\phi = 2kd = 4\pi d/\lambda = 4\pi df_0/c = 2\omega_0/c.$$

Thus, the form of the received signal is

$$u(t) = \sigma \exp(j[-\omega_0(t - 2d/c)]) \sum_{m=0}^{M-1} v_p(t - 2d/c - mT_r)$$

where  $\sigma$  is the reflection coefficient. Without loss of generality, we can consider only one component of the received signal:

$$q(m, t) = \sigma \exp(j\omega_0 2d/c) \exp(-j2\pi Bf_r(t - mT_r)2d/c).$$

A two-dimensional discrete signal is obtained by sampling in time with  $t - mT_r = nT_s$ :

$$q(m, n) = \sigma \exp(j\omega_0 2d/c) \exp(-j2\pi Bf_r n T_s 2d/c).$$

### III. FOURIER TRANSFORM IN ISAR

The two-dimensional (2D) Fourier transform of the received signal is

$$Q(m', n') = \sum_{m=0}^{M-1} \sum_{n=0}^{N-1} q(m, n) \exp\left[-j2\pi\left(\frac{mm'}{M} + \frac{nn'}{N}\right)\right],$$

where time is discretized such that  $t - mT_r = nT_s$ . The periodogram

$$P(m', n') = |Q(m', n')|^2,$$

represents an ISAR image. In order to analyze cross-range nonstationarities in the Fourier transform, we consider only the Doppler component part of the received signal (the  $p$ -th point scatterer), as it is usually done in the literature on ISAR,

$$e_p(t) = \sigma_p \exp[j2\omega_0 d_p(t)/c]. \quad (3)$$

The Fourier transform of  $e_p(t)$  produces

$$E_p(\omega) = \int_{-\infty}^{\infty} w(t) e_p(t) \exp(-j\omega t) dt,$$

where  $w(t)$  is the window defining the considered time interval (CIT). In order to simplify the notation we will just omit the index  $p$ . For time-varying  $d(t)$  we can write a Taylor series expansion of  $d(t)$  around  $t = 0$ :

$$d(t) = d_0 + d'(0)t + \frac{1}{2}d''(0)t^2 + \dots = \sum_{n=0}^{\infty} \frac{1}{n!} d^{(n)}(0)t^n, \quad (4)$$

where  $d^{(n)}(0)$  is the  $n$ -th derivative of the distance at  $t = 0$  and  $2\omega_0 d'(0)/c = \Delta\omega_d$ . The Fourier transform (FT) of (3) with (4) is of the form

$$E(\omega) = \int_{-\infty}^{\infty} w(t) \exp[j \frac{2\omega_0}{c} \sum_{n=0}^{\infty} \frac{1}{n!} d^{(n)}(0)t^n - j\omega t] dt, \quad (5)$$

Now, by omitting the constant term  $d(0)$  and shifting  $2\omega_0 d'(0)/c = \Delta\omega_d$  into the second exponential term we get

$$E(\omega) = W(\omega - \Delta\omega_d) *_{\omega} FT \left( \exp \left[ j \frac{2\omega_0}{c} \sum_{n=2}^{\infty} \frac{1}{n!} d^{(n)}(0)t^n \right] \right), \quad (6)$$

where  $*_{\omega}$  denotes convolution in frequency. Thus, the Fourier transform is located at and around the Doppler shift  $\omega = \Delta\omega_d$ . It is spread by the factor

$$S_{spread}(\omega) = FT \left( \exp \left[ j \frac{2\omega_0}{c} \sum_{n=2}^{\infty} \frac{1}{n!} d^{(n)}(0)t^n \right] \right).$$

This factor depends on the derivatives of the distance, starting from the second order (first order derivative of the Doppler shift), i.e., the spread factor depends on

$$s_f(t) = \frac{1}{2} d''(0)t^2 + \frac{1}{6} d'''(0)t^3 + \dots$$

It can significantly degrade the periodogram image  $P(\omega) = |E(\omega)|^2$ . This means that in the Fourier transform-based image the spreading terms started from the second derivative  $d''(0)$ . The goal of the ISAR signal processing is to obtain the focused radar image, i.e., to remove the influence of the second and higher terms in signal phase of each component.

### IV. S-METHOD-BASED IMPROVEMENT OF THE RADAR IMAGES

In this section we will present a method for improvement of images blurred due to the long CIT and/or nonuniform movement. Instead of using the Fourier transform (periodogram), we use the S-method (SM) defined by [4,6]

$$SM(\omega) = \frac{1}{\pi} \int_{-\infty}^{\infty} E(\omega + \theta) E^*(\omega - \theta) d\theta. \quad (7)$$

This method can improve the image concentration in a numerically very simple and efficient way. Namely, by replacing  $E(\omega)$  from (5) into (7) we get

$$\begin{aligned} SM(\omega) &= \frac{1}{\pi} \int_{-\infty}^{\infty} \int_{-\infty}^{\infty} \int_{-\infty}^{\infty} w(t_1) w(t_2) \\ &\times \exp(j \frac{2\omega_0}{c} \sum_{n=0}^{\infty} \frac{1}{n!} d^{(n)}(0)t_1^n - j \frac{2\omega_0}{c} \sum_{n=0}^{\infty} \frac{1}{n!} d^{(n)}(0)t_2^n) \\ &\times \exp[-j(\omega + \theta)t_1] \exp[-j(\omega + \theta)t_2] dt_1 dt_2 d\theta \end{aligned}$$

The part of integrand depending on  $\theta$  is  $\exp[-j\theta(t_1 + t_2)]$ . Integration over  $\theta$  results in  $2\pi\delta(t_1 + t_2)$ . Integration of a function  $g(t_1)g(t_2)\delta(t_1 + t_2)$  over  $t_1$  results in the function  $g(t)g(-t)$  for  $t_1 = -t_2 = t$ . From the previous equation it means that we obtain

$$SM(\omega) = W_e(\omega - \Delta\omega_d) *_{\omega} FT \left( \exp \left[ j \frac{2\omega_0}{c} \left( \frac{1}{3!} d'''(0)t^3 + \dots \right) \right] \right)$$

where similar calculations as in (5)-(6) are performed. The S-method-based image is located at the same position in Doppler space as the Fourier transform image,  $\omega = \Delta\omega_d$ , but with the spreading term

$$S_{\text{spread}}(\omega) = FT \left( \exp \left[ j \frac{2\omega_0}{c} \left( \frac{1}{3!} d'''(0)t^3 + \dots \right) \right] \right).$$

Its exponent starts from the third derivative  $d'''(0)$

$$s_f(t) = \frac{1}{6} d'''(0)t^3 + \frac{1}{120} d^{(5)}(0)t^5 + \dots$$

This means that the S-method has the ability to automatically compensate for quadratic and all even higher-order terms in phase. Recall that in the Fourier transform-based image the spreading terms started from the second derivative  $d''(0)$ . It means that in the S-method, the points with linear Doppler changes,

$$\frac{2\omega_0}{c} d'(t) = \Delta\omega_d(t) = \Delta\omega_d + at,$$

will be fully concentrated without any spread, since here  $s_f(t) = 0$ . Thus, targets with constant acceleration will undergo full motion compensation and their point-scatterers will each be localized. Note that  $W_e(\omega)$  is the Fourier transform of window  $w(t/2)w^*(-t/2)$  while  $\Delta\omega_d$  without argument denotes the constant part of  $\Delta\omega_d(t)$ , i.e.,  $\Delta\omega_d = \Delta\omega_d(0)$ . It should also be noted that the source of the quadratic term can come from not only acceleration, but also non-uniform rotational motion and the cosine term in wide-angle imaging.

#### A. Numerical implementation

The discrete version of (7) is

$$SM(k) = \sum_{i=-L}^L E(k+i)E^*(k-i)$$

or

$$SM_L(k) = SM_{L-1}(k) + 2 \operatorname{Re}\{E(k+L)E^*(k-L)\}, \quad (8)$$

with  $SM_0(k) = |E(k)|^2$  being the standard Fourier transform-based representation. Therefore, the S-method improvement

can be achieved starting with the radar image, with additional simple matrix calculation according to Equation (8).

## V. EXPERIMENTAL DATA

An ISAR experiment is set up to examine the distortion of ISAR images due to a time-varying rotational motion. A 2-dimensional delta-wing shaped target, the target motion simulator (TMS), is built for the ISAR distortion experiments [8]. The target has a length of 5 m on each of its three sides. Six trihedral reflectors are mounted on the TMS as scattering centres of the target; all the scatterers are located on the  $x$ - $y$  plane. They are designed to always face towards the radar as the TMS rotates. The TMS target is set up so that it rotates perpendicular to the radar line of sight. Note that one corner reflector is placed asymmetrically to provide a relative geometric reference of the TMS target. A time-varying rotational motion is introduced by a programmable motor drive.

The delta-wing data was collected using an X-band radar operating at a center frequency of 10.1 GHz with 300 MHz bandwidth and a range resolution of 0.5 m. The PRF is 2 kHz. Each HRR profile is generated in 0.5 ms and each profile has 41 range bins. The total data set contains 60,000 HRR profiles. The delta-wing is at a range of 2 km and is rotating at 2 degrees/second.

Since the entire data set consists of 60,000 pulses in the cross-range, it can be "cut" into different size imaging intervals with each of the intervals displaying a different amount of motion error. This is the approach used in this paper. Figs. 1-3 show ISAR images from three different imaging intervals. The smallest interval consists of 1024 pulses in the cross-range, which corresponds to a CIT of 0.512 seconds (Fig. 1) and the largest interval consists of 4096 pulses, which corresponds to 2.048 seconds (Fig. 3). Fig. 2 shows the ISAR image from 2048 pulses, which corresponds to a CIT of 1.024 seconds. The Figures' leftmost columns show the Fourier transform-based representations and their rightmost columns show the S-method-based representations. Since significant phase errors due to nonuniform motion exist in the data, the Fourier transform-based images are blurred in the cross-range dimension. This is most evident in Figs. 3a, 3c, 3e and 2a where it is not possible to locate individual reflectors as some are severely blurred. In each of the S-method-based images, the cross-range smearing is significantly reduced resulting in a dramatic improvement in image quality. The images are now focused and the six reflectors are visible.

## VI. CONCLUSION

In this paper, we present the S-method based approach to real-time motion compensation, image formation and image enhancement of moving targets in ISAR. The commonly used technique for ISAR signal analysis is a two-dimensional Fourier transform, which results in an image of the target's reflectivity mapped onto a range and cross-range plane. However, in cases where the line-of-sight projections of the target's point velocities change or there is uncompensated movement within the coherent integration time, the Fourier transform produces blurred images. For target recognition

applications, mainly those in military surveillance and reconnaissance operations, a blurred ISAR image has to be refocused quickly so that it can be used for real-time target identification.

We present an effective quadratic time-frequency representation, the S-method. This approach performs better than the Fourier transform method by drastically improving images of fast manoeuvring targets. These advantages are a result of the S-method's ability to automatically compensate for quadratic and all even higher-order phase terms. Thus, targets with constant acceleration will undergo full motion compensation and their point-scatterers will each be localized.

It should be noted that the source of the quadratic term can come from not only acceleration, but also non-uniform rotational motion and the cosine term in wide-angle imaging. The method is also computationally simple, requiring only slight modifications to the existing Fourier transform-based algorithm. The effectiveness of the S-method is demonstrated through application to experimental data sets.

This paper demonstrates that the S-method can be applied to real-time target identification in ISAR systems. This work is especially pertinent to the ISAR imaging capability in military intelligence, surveillance and reconnaissance operations.

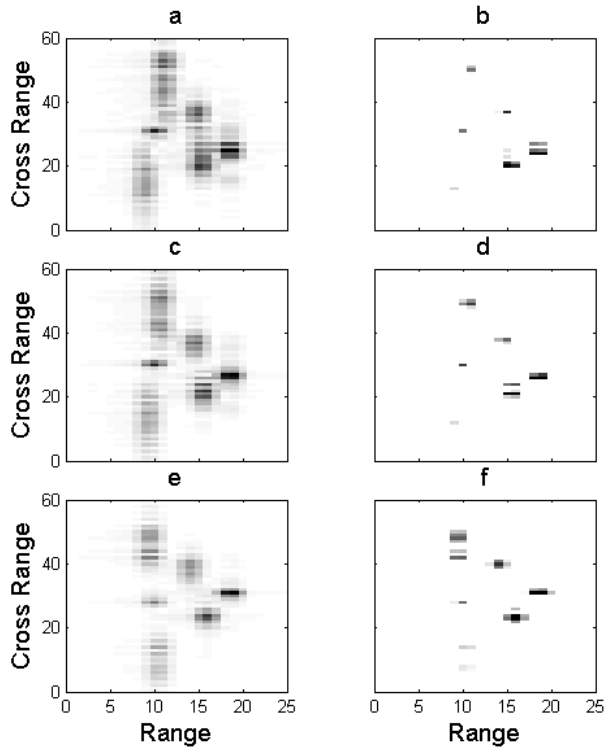


Figure 1. ISAR images from experimental delta-wing data. First column contains Fourier transform-based images and second column contains S-method-based ISAR images. Each image is zoomed in on the target for clear presentation.

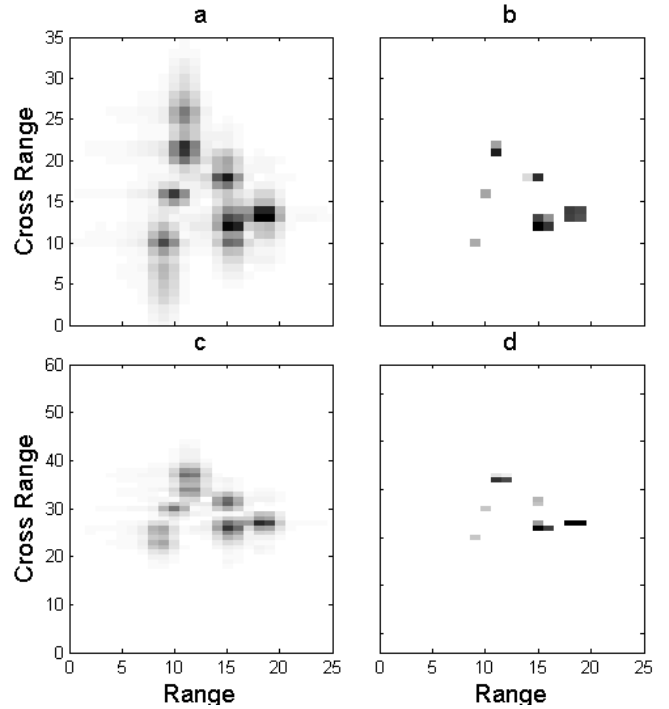


Figure 2. ISAR images from experimental delta-wing data. First column contains Fourier transform-based images and second column contains S-method-based ISAR images. Each image is zoomed in on the target for clear presentation.

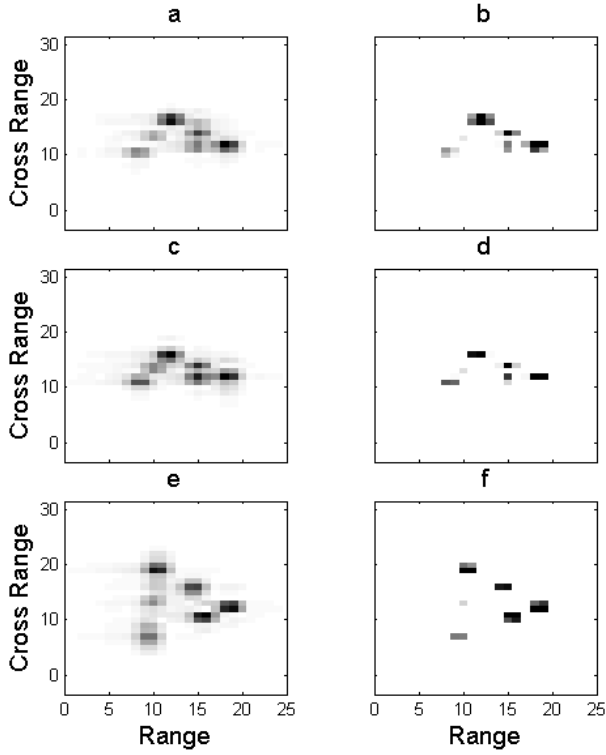


Figure 3. ISAR images from experimental delta-wing data. First column contains Fourier transform-based images and second column contains S-method-based ISAR images. Each image is zoomed in on the target for clear presentation.

## REFERENCES

- [1] Lj. Stanković, T. Thayaparan, and M. Daković, "Improvement of the Fast Moving Targets Presentation in ISAR by Using the S-Method," 13th European Signal Processing Conference EUSIPCO 2005, Antalya, Turkey.
- [2] T. Thayaparan, Lj. Stanković, and M. Daković, "Focusing distorted ISAR images using the s-method," pp. 121-125, May 7, IEEE CCECE 2006 Conference, Ottawa, Canada.
- [3] Lj. Stanković, "The auto-term representation by the reduced interference distributions: The procedure for a kernel design," IEEE Trans. on Signal Processing, 1996, Vol. 44, No. 6, pp. 1,557-1,564.
- [4] Lj. Stanković, "A method for time-frequency analysis," IEEE Trans. Signal Processing, 1994, Vol. 42, pp. 225-229.
- [5] Lj. Stanković and J.F. Böhme, "Time-frequency analysis of multiple resonances in combustion engine signals," Signal Processing, 1999, Vol. 79, No. 1, pp. 15-28.
- [6] L.L. Scharf, and B. Friedlander, "Toeplitz and Hankel kernels for estimating time-varying spectra of discrete-time random processes," IEEE Trans. Signal Process., 2001, Vol. 49, pp. 179-189.
- [7] V.C. Chen and H. Ling, Time-frequency transforms for radar imaging and signal analysis, Artech House, Boston, USA, 2002
- [8] T. Thayaparan, G. Lampropoulos, S.K. Wong, and E. Riseborough, "Application of adaptive joint time-frequency algorithm for focusing distorted ISAR images from simulated and measured radar data," IEE Proc. Radar, Sonar Navig., 2003, Vol. 150, No. 4, pp. 213-220.